A Mechanical Fourier Series Generator: An Exact Solution

Izhak Bucher
Mechanical Engineering,
Technion,
Haifa 32000, Israel
e-mail: bucher@technion.ac.il

A vibrating system is constructed such that its natural frequencies are exact integer multiples of a base frequency. This system requires little energy to produce a periodic motion whose period is determined by the base frequency. The ability to amplify integer multiples of a base frequency makes this device an effective mechanical Fourier series generator. The proposed topology makes use of symmetry to assign poles and zeros at optimal frequencies. The system zeros play the role of suppressing the energy at certain frequencies while the poles amplify the input at their respective frequencies. An exact, non-iterative procedure is adopted to provide the stiffness and mass values of a discrete realization. It is shown that the spatial distributions of mass and stiffness are smooth; thus it is suggested that a continuous realization of a mechanical Fourier series generator is a viable possibility. A laboratory experiment and numerical examples are briefly described to validate the theory. [DOI: 10.1115/1.3085892]

1 Introduction

Mechanical structures consume the smallest amount of energy for a given displacement when they are operated at resonance [1,2]. Indeed, many engineering designs make use of an oscillator to produce sinusoidal motions whereby the stiffness and the mass distribution are tuned such that a particular natural frequency coincides with the desired excitation and response frequencies.

A problem arises when one wishes to design an energy efficient mechanical system that produces periodic, nonsinusoidal motion described by a Fourier series of the form

$$x(t) = \sum_n C_n \cos(n\omega_0 t + \beta_n) \tag{1}$$

where n can attain even or odd values (or both) depending on the motion that one seeks to represent. In any case, the series is finite and the highest term (highest harmonic) equals $N+1$.

Equation (1) describes a periodic function, which is completely determined by the coefficients C_n and β_n and it describes the desired oscillation pattern of a structural element within an elastic structure. The number of terms, $N+1$, is related to the number of degrees of freedom in the vibrating system, which is shown schematically in Fig. 1. Indeed, from Fig. 1 it is clear that this work restricts itself to systems whose topology consists of a series of masses and springs. This topology has been studied extensively in literature, and this work is based on some previously obtained results, e.g., Refs. [3,4]. Structural modifications leading to the assignment of zeros and natural frequencies have been dealt with in the past [5–7], but these methods have limited capabilities because they are implemented on existing structures with a predetermined topology.

Although damping is neglected in the present analysis, it is implicitly assumed that the final structure does contain a very small amount of damping. This level of damping is sufficiently small to affect the natural frequencies by a negligible amount and still it restricts the vibration amplitudes even when the excitation frequencies coincide with the natural frequencies. Damping does cause a phase shift, but this can be rectified by pre-adjusting the excitation's phase [14].

A structure that draws a minimal amount of energy, or equivalently, uses the smallest possible magnitude of excitation levels, should be compliant at the frequencies $n\omega_0$, and therefore these must all be natural frequencies, i.e., $\omega_n = n\omega_0$ [2]. It is possible to set the natural frequencies at any multiple of ω_0, but for the sake of brevity, only odd multiples are discussed in this work and in the examples.

The task of designing a mechanical structure, which is compliant at the frequencies $n\omega_0$, proves generally difficult, but for a class of discrete systems this problem seems to have been solved [3,4]. Often, it is also necessary to assign the frequencies [5–7] at which the system is not compliant, i.e., the system zeros [5,8] or antiresonance frequencies [9], so that the designed structure is robust and it attenuates certain spectral contents.

The problem at hand is an inverse problem where the relevant parameters, e.g., mass and stiffness, need to be recovered from some required spectra.

In this work, the proposed topology consists of a series of masses and springs that produce linear or angular (torsional) motion. This topology has been studied in the past and it gives rise to a tridiagonal stiffness matrix often addressed as Jacobi matrix [4]. Reference [10] has coined the term oscillatory matrices, and numerous authors, some of which are cited in a survey [3], and a book [4], following their footsteps, have addressed the reconstruction of Jacobi matrices and mass and stiffness values from a given desired spectrum. A much cited work by Boley and Golub [3] surveys the connections between the theory of orthogonal polynomials, in particular, Sturm sequence (based on the Sturm theorem dated 1835), and between matrix eigenvalue problems. The well known Lanczos algorithm [11] presenting the important matrix algorithm is the main tool in performing this reconstruction. Reference [12] has made an important contribution with which the Jacobi matrix can now be reconstructed from a given spectrum under two interlacing spectra, see also Ref. [10]. A symmetric topology that gives rise to persymmetric matrices (see Refs. [13,4]) conforms to the abovementioned matrix reconstruction theories. These theories are being used in the sequel to develop a matrix reconstruction algorithm from which the topology of the vibrating system is found. The individual values of mass and spring elements are computed, so a physical system can thus be formed.

The present theory and its derivatives were used to produce working systems [14,15]. At that time, the theory was not fully developed and therefore this paper fills the gap.

This paper begins with an introduction and a survey. Section 2 provides a description of the problem and develops the necessary theory and main ideas while indicating the relevant references. In Sec. 3, the inverse problem's solution stages are outlined and ref-

Contributed by the Technical Committee on Vibration and Sound of ASME for publication in the JOURNAL OF VIBRATION AND ACOUSTICS. Manuscript received July 1, 2008; final manuscript received January 6, 2009; published online April 23, 2009. Assoc. Editor: Jean-Claude Golinval.

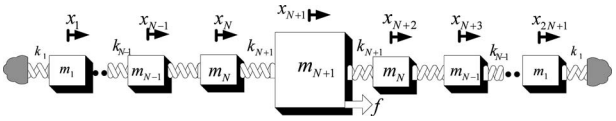

Fig. 1 Topology of the spring mass series

erences are being made to the theory and to existing algorithms that were used. Some computer code and pseudocode implementing the algorithm are provided too. Several examples are described in Sec. 4 from small discrete systems through a system with many degrees of freedom to a continuous structure that was realized in the laboratory.

2 Problem Definition and Proofs

Consider a symmetric vibrating system consisting of a spring mass series, as shown in Fig. 1. The system has $2N+1$ degrees of freedom and it is symmetric around the center mass (m_{N+1}).

The steady state response, at the middle mass, to sinusoidal excitation, $f=Q_0 \sin \omega t$, acting at the same point, can be written as [16,1]

$$x_{N+1}(t) = e_{N+1}^T (K - \omega^2 M)^{-1} e_{N+1} Q_0 \sin \omega t \overset{\Delta}{=} \alpha(\omega) Q_0 \sin \omega t \quad (2)$$

where e_{N+1} is the $(N+1)$th column of the identify matrix, $K, M \in \mathbb{R}^{(2N+1)\times(2N+1)}$ are the stiffness and mass matrices, $\alpha(\omega)$ is the point receptance at the middle mass, and Q_0 is the force amplitude.

Having predetermined values for the center mass m_{N+1} and for the basis frequency ω_0, the current problem seeks the mass $\{m_i\}_{i=1}^{N}$ and stiffness $\{k_i\}_{i=1}^{N+1}$ elements for which the receptance has the form

$$\alpha(\omega) = \gamma_0 \frac{\prod_{n=1}^{N} ((2n)^2 \omega_0^2 - \omega^2)}{\prod_{n=1}^{N_{N+1}} ((2n-1)^2 \omega_0^2 - \omega^2)} \quad (3)$$

Examination of Eq. (3) reveals that the receptance becomes infinitely large at odd multiples of the basis frequency, i.e., at discrete excitation frequencies where $\omega=(2n-1)\omega_0$. In addition, the receptance becomes zero at the midpoint between the maxima, i.e., at excitation frequencies where $\omega=2n\omega_0$. γ_0 is a scaling factor depending on the force and sensor transducers.

It turns out that this goal can be achieved by employing known algorithms that assign the natural frequencies of two subsystems of Fig. 1. These subsystems are shown in Fig. 2.

This decomposition is central to the construction of the "mechanical Fourier series generator" (MFSG), as described in Sec. 2.1.

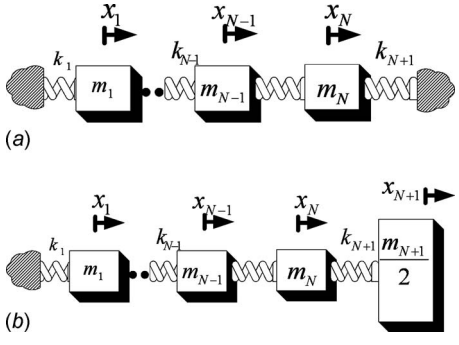

Fig. 2 Right: A dissected left half of Fig. 1 with *N*+1DOF; left: left half of Fig. 1, clamped at the middle thus leaving *N* DOF

2.1 Decomposition of the Symmetric System: Persymmetry. In this subsection, it is shown that the spectra of the subsystems in Fig. 2 determine the poles and zeros of the receptance $\alpha(\omega)$. It will be shown that one can assign the spectra of these two subsystems to produce the required frequency response, which is given in Eq. (3).

Owing to the symmetry of Fig. 1, the mass and stiffness matrices in Eq. (2) can be decomposed into submatrices. These submatrices are a manifestation of Fig. 2. As proved below, they are jointly equivalent to the system in Fig. 1.

Define $J_N \in \mathbb{R}^{N\times N}$ as a reflection matrix having ones on the secondary diagonal [13]. The operation $J_N x$ reverses the order of the elements in the vector—x.

It can be shown that both the mass and stiffness of Fig. 1 are persymmetric, i.e.,

$$K = \begin{bmatrix} K_0 & -k_{N+1}e_N & 0_N \\ -k_{N+1}e_N^T & 2k_{N+1} & -k_{N+1}e_N^T J_N \\ 0_N & -k_{N+1}e_N J_N & J_N K_0 J_N \end{bmatrix}, \quad M = \begin{bmatrix} M_0 & 0 & 0_N \\ 0 & m_{N+1} & 0 \\ 0_N & 0 & J_N M_0 J_N \end{bmatrix} \quad (4)$$

Here 0_N is a $N\times N$ zero matrix.

The operations $K=J_{2N+1}KJ_{2N+1}$ and $M=J_{2N+1}MJ_{2N+1}$ flip both matrices around the two main diagonals showing that they are indeed persymmetric. Equation (4) makes use of partial mass and stiffness to represent the left system in Fig. 2:

$$M_0 = \begin{bmatrix} m_1 & 0 & \cdots & 0 \\ 0 & m_2 & \ddots & \vdots \\ \vdots & \ddots & \ddots & 0 \\ 0 & \cdots & 0 & m_N \end{bmatrix}, \quad K_0 = \begin{bmatrix} k_1 + k_2 & -k_2 & \cdots & 0 \\ -k_2 & k_2 + k_3 & \ddots & \vdots \\ \vdots & \ddots & \ddots & -k_N \\ 0 & \cdots & -k_N & k_N + k_{N+1} \end{bmatrix} \in \mathbb{R}^{N\times N} \quad (5)$$

With these definitions it is now possible to develop an expression for the receptance.

From matrix and linear systems theories it is possible to write

$$\alpha(\omega) = e_{N+1}^T (K - \omega^2 M)^{-1} e_{N+1} = \frac{e_{N+1}^T \operatorname{adj}(K - \omega^2 M) e_{N+1}}{\det(K - \omega^2 M)} \quad (6)$$

or, using Eq. (4),

$$\alpha(\omega) = \frac{\det(K_0 - \omega^2 M_0) \det(J_{N+1} K_0 J_{N+1} - \omega^2 J_{N+1} M_0 J_{N+1})}{\det(K - \omega^2 M)} \quad (7)$$

Now, since J_{N+1} is orthonormal, and due to persymmetry, Eq. (7) can be simplified into

$$\alpha(\omega) = \frac{\det(K_0 - \omega^2 M_0)^2}{\det(K - \omega^2 M)} \quad (8)$$

Define λ_n, ϕ_n as the solutions of

$$(K - \lambda_n M)\phi_n = 0, \quad n = 1, \ldots, 2N+1 \quad (9)$$

And μ_n as the solutions of

$$(K_0 - \mu_n M_0) a_n = 0, \quad n = 1, \ldots, N \quad (10)$$

It is now possible to express the receptance in terms of the natural frequencies of the two subsystems in Fig. 2:

$$\alpha(\omega) = \gamma_0 \frac{\prod_{n=1}^{N}(\mu_n - \omega^2) \prod_{n=1}^{N}(\mu_n - \omega^2)}{\prod_{n=1}^{2N+1}(\lambda_n - \omega^2)} \tag{11}$$

Having established these relations it remains to assign

$$\mu_n = 2n\omega_0, \quad n = 1, \ldots, N$$
$$\lambda_n = n\omega_0, \quad n = 1, \ldots, 2N+1 \tag{12}$$

With this assignment, some of the poles in Eq. (11) cancel out with the zeros to yield Eq. (3).

It is now required to study the eigenvalues and eigenvectors of the vibrating system whose mass and stiffness are defined in Eqs. (4) and (5) and to find a method to assign Eq. (12).

2.2 Eigenvectors and Eigenvalues of a Symmetric Spring Mass Series. It will now be shown how the symmetric system in Fig. 1 can be represented by the two systems in Fig. 2. Defining a transformation matrix L,

$$L = \frac{1}{\sqrt{2}} \begin{bmatrix} I_N & 0 & I_N \\ 0 & 1 & 0 \\ J_N & 0 & -J_N \end{bmatrix} \tag{13}$$

the mass and stiffness can be transformed in the spirit of Ref. [13] into

$$\tilde{K} \overset{\Delta}{=} L^T K L = \begin{bmatrix} K_0 & -k_{N+1}e_N & 0 \\ -k_{N+1}e_N^T & k_{N+1} & 0 \\ 0 & 0 & K_0 \end{bmatrix},$$
$$\tilde{M} = L^T M L = \begin{bmatrix} M_0 & 0 & 0 \\ 0 & \frac{1}{2}m_{N+1} & 0 \\ 0 & 0 & M_0 \end{bmatrix} \tag{14}$$

The transformed matrices have two sets of eigenpairs. The first one, (λ, a), is found from the lower diagonal block, providing N eigenvalues, via

$$\mu M_0 a = K_0 a, \quad a \in \mathbb{R}^N \tag{15}$$

Since the eigenvalues in Eq. (15) are distinct [10], the N related eigenvectors must be a linear combination of the third column of Eq. (13) and therefore these eigenvectors of Eq. (9) have the form

$$\phi = \begin{bmatrix} I & 0 & I \\ 0 & 1 & 0 \\ J_N & 0 & -J_N \end{bmatrix} \begin{pmatrix} 0 \\ 0 \\ a \end{pmatrix} = \begin{pmatrix} I \\ 0 \\ -J_N \end{pmatrix} a = \begin{pmatrix} a \\ 0 \\ -J_N a \end{pmatrix} \tag{16}$$

Equation (16) clearly shows that these modes have a nodal point at the middle mass and are antisymmetric, i.e., $\phi[N+1]=0$ and $\phi[i]=-\phi[N+2-i]$.

The eigenvalues, being a subset of those obtained from Eq. (9), belong to the eigenvectors with a nodal point at the middle, for these

$$\lambda_{2n} = \mu_n, \quad n = 1, \ldots, N \tag{17}$$

i.e., the even numbered eigenvalues of Eq. (9).

The remaining $N+1$ eigenpairs are the solution of the remaining diagonal blocks in Eq. (14):

$$\begin{bmatrix} K_0 & -k_{N+1}e_N \\ -k_{N+1}e_n^T & k_{N+1} \end{bmatrix} \begin{pmatrix} b \\ c \end{pmatrix} = \lambda \begin{bmatrix} M_0 & 0 \\ 0 & \frac{1}{2}m_{N+1} \end{bmatrix} \begin{pmatrix} b \\ c \end{pmatrix},$$
$$b \in \mathbb{R}^N, \quad c \in \mathbb{R} \tag{18}$$

As before, the eigenvectors are a linear combination of the two leftmost columns of Eq. (13),

$$\phi = \begin{bmatrix} I & 0 & I \\ 0 & 1 & 0 \\ J_N & 0 & -J_N \end{bmatrix} \begin{pmatrix} b \\ c \\ 0 \end{pmatrix} = \begin{pmatrix} b \\ c \\ J_N b \end{pmatrix} \tag{19}$$

Equation (19) shows that these modes are symmetric, i.e., $\phi[i] = \phi[N+2-i]$, $i=1, \ldots, N+1$.

To summarize, the recent development stated that the system in Fig. 1 (and Eq. (9)) has two types of eigenvectors (modes of vibration). There are N antisymmetric modal vectors for which the center mass does not move; these have the eigenvalues denoted by μ_n. In addition, there are $N+1$ eigenvectors that are symmetric around the center mass; these are denoted by λ_{2n-1}. Both are eigenpairs of the mass and stiffness in Eq. (4). This fact reported in the past leads to the desired form of the receptance.

Now, using Eq. (17), it can be shown that several terms cancel out in Eq. (11) to yield

$$\alpha(\omega) = \beta_0 \frac{\prod_{n=1}^{N}(\mu_n - \omega^2)}{\prod_{n=1}^{N+1}(\lambda_{2n-1} - \omega^2)} = \beta_0 \frac{\prod_{n=1}^{N}(\lambda_{2n} - \omega^2)}{\prod_{n=1}^{N+1}(\lambda_{2n-1} - \omega^2)} \tag{20}$$

Enforcing Eq. (12), Eq. (20) will become identical to the desired form, i.e., to Eq. (11).

It is worth mentioning that the even eigenvalues are zeros of the transfer function in this case.

Recalling the fact that μ_n $(=\lambda_{2n})$ and λ_{2n-1} (strictly) interlace [4], it is indeed possible to assign the desired values to the natural frequencies, as indicated in Eq. (12). This subproblem has already been solved in literature [12,3], and the algorithm with which the particular values of this problem are obtained is outlined below. The algorithm is implemented in a MATLAB™ program that makes use of symbolic computation and is provided in the Appendixes.

3 Solving the Inverse Problem

Having established that the proposed topology in Fig. 1 can indeed produce the desired frequency response once the matrices in Eq. (4) are assigned the desired eigenvalues, it now remains to find the mass and stiffness elements for which these conditions exist.

Denoting

$$K_1 \overset{\Delta}{=} \begin{bmatrix} K_0 & -k_{N+1}e_N \\ -k_{N+1}e_N^T & k_{N+1} \end{bmatrix}, \quad M_1 \overset{\Delta}{=} \begin{bmatrix} M_0 & 0 \\ 0 & \frac{1}{2}m_{N+1} \end{bmatrix} \in \mathbb{R}^{(N+1)\times(N+1)} \tag{21}$$

by defining

$$\phi = M_1^{-1/2} u \tag{22}$$

and substituting into Eq. (9), an equivalent Jacobi (tridiagonal) matrix B with identical eigenvalues to Eq. (9) can be defined [3,4,12] as

$$\overset{\Delta}{B}=M_1^{-1/2}K_1M_1^{-1/2}=\begin{bmatrix} a_1 & -b_1 & & \\ -b_1 & a_2 & -b_2 & \\ & -b_2 & a_3 & \ddots \\ & & \ddots & \ddots \end{bmatrix}\in\mathbb{R}^{(N+1)\times(N+1)} \tag{23}$$

where (see Ref. [4])

$$K_1=E^T\begin{bmatrix} k_1 & 0 & \cdots & 0 \\ 0 & k_2 & \ddots & \vdots \\ \vdots & & \ddots & 0 \\ 0 & \cdots & 0 & k_{N+1} \end{bmatrix}E,\quad \overset{\Delta}{E}=\begin{pmatrix} 1 & -1 & 0 & 0 \\ 0 & 1 & -1 & 0 \\ 0 & 0 & 1 & \ddots \\ 0 & 0 & 0 & \ddots \end{pmatrix} \tag{24}$$

Observing that M_0, K_0 can be obtained from M_1, K_1 by deleting the last row and column, the method that reconstructs B and the system in Fig. 1 is, in fact, available in literature [3,12,4].

The reconstruction method makes use of pre-assigned values $\{\lambda_n=n\omega_0,\ n=1,\ldots,2N+1\}$, m_{N+1}, and ω_0.

The first step reconstructs the $(N+1)$th left eigenvector of B, as explained below.

Use is being made of the identity (see proof in Appendix A and Ref. [4])

$$u_i^2(N+1)=\frac{\prod_{k=1}^{N}(\lambda_{2i-1}-\mu_k)}{\prod_{\substack{k=1\\k\neq i}}^{N+1}(\lambda_{2i-1}-\lambda_{2k-1})},\quad i=1,\ldots,N+1 \tag{25}$$

In the present case, this expression can be simplified into

$$\begin{aligned} u_i^2(N+1)&=\frac{\prod_{k=1}^{N}((2i-1)^2\omega_0^2-4k^2\omega_0^2)}{\prod_{\substack{k=1\\k\neq i}}^{N+1}((2i-1)^2\omega_0^2-(2k-1)^2\omega_0^2)} \\ &=\frac{\prod_{k=1}^{N}((2i-1)^2-4k^2)}{\prod_{\substack{k=1\\k\neq i}}^{N+1}((2i-1)^2-(2k-1)^2)} \end{aligned} \tag{26}$$

It is important to observe that $u_i^2(N+1)$ is independent of ω_0. Equation (26) remains unchanged as long as the eigenvalues are an integer multiple of λ_1.

3.1 Reconstruction Algorithm. The reconstruction algorithm consists of three steps.

(i) Given ω_0, N, use Eq. (26) to compute $u_i(N+1)$, $i=1,\ldots,N+1$.
(ii) Run the Lanczos algorithm, described in Appendix B, to retrieve B.
(iii) Run the algorithm described below to recover M and K and m_i, k_i.

3.1.1 Algorithm to Recover M and K From B . Define

$$P\triangleq\operatorname{diag}(p)=\operatorname{diag}\left(\sqrt{m_1}\quad\sqrt{m_2}\quad\cdots\quad\sqrt{m_{N+1}/2}\right)^T\in\mathbb{R}^{(N+1)\times(N+1)} \tag{27}$$

It can be shown that [4]

$$Bp=\frac{k_1}{\sqrt{m_1}}e_1 \tag{28}$$

Solving $Bt=e_1$ for t, it is possible to obtain a vector proportional to p:

$$t=\frac{\sqrt{m_1}}{k_1}\left(\sqrt{m_1}\quad\sqrt{m_2}\quad\cdots\quad\sqrt{m_{N+1}/2}\right)^T=\frac{\sqrt{m_1}}{k_1}p^T \tag{29}$$

Squaring Eq. (29),

$$\frac{m_1}{k_1^2}M_1=[\operatorname{diag} t]^2 \tag{30}$$

Ignoring the scaling factor for now, one can combine the outcome of Eq. (30) with Eq. (24) to compute

$$[\operatorname{diag} t]B[\operatorname{diag} t]=\frac{m_1}{k_1^2}K_1 \tag{31}$$

Having recovered M_1, K_1, up to a scaling factor, Eq. (4) can be used to construct M and K.

The individual but scaled springs are computed from Eq. (24) via

$$\begin{bmatrix} \alpha_1 & & & \\ & \alpha_2 & & \\ & & \ddots & \\ & & & \alpha_{N+1} \end{bmatrix}=E^{-T}K_1E^{-1} \tag{32}$$

Now, the scaling factor is eliminated by assigning values for the middle mass and the base frequency of $\bar{m}_{N+1}$ and $\bar{\omega}_0$.

The final values of the mass and spring elements, $\bar{m}_i, \bar{k}_i$, are computed with

$$\bar{m}_i=t_i^2\frac{\bar{m}_{N+1}}{2t_{N+1}^2},\quad i=1,\ldots,N,\quad \bar{k}_i=\alpha_i\frac{\bar{\omega}_0^2}{2t_{N+1}^2},\quad i=1,\ldots,N+1 \tag{33}$$

The entire calculation process is formulated in a MATLAB™ program provided in the Appendixes.

4 Solving the Inverse Problem: Examples

Consider using the proposed algorithm to produce an approximation of a square-wave-like motion by driving the mechanical system at several natural frequencies simultaneously. The truncated Fourier series representation of a square wave is

$$x_{N+1}(t)=\sum_{n=1}^{N+1}\frac{\sin(2n-1)\omega_0 t}{(2n-1)} \tag{34}$$

Having frequency terms at odd multiples of the basis frequency, it is possible to employ the proposed algorithm with a different number of terms. Sample solutions are tabulated below.

The eigenpairs for the case where $2N+1=5$, as computed by the program in the Appendixes, are

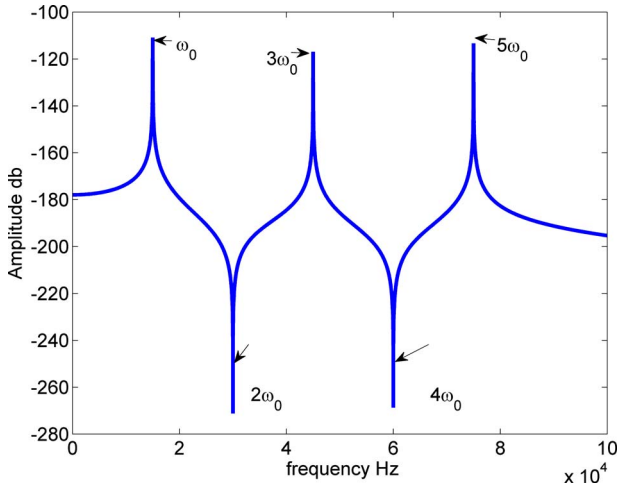

Fig. 3 Frequency response magnitude for a $2N+1=5$DOF structure scaled for $\omega_0=15{,}000$ Hz

$$\text{diag}\,\lambda = \omega_0^2\,\text{diag}\begin{pmatrix}1 & 2^2 & 3^2 & 4^2 & 5^2\end{pmatrix}, \tag{35}$$

$$\Phi = \begin{pmatrix} 1 & -\frac{3}{2} & -\frac{9}{4} & 1 & 1 \\ \frac{4}{3} & -1 & 1 & -2 & -4 \\ \frac{10}{7} & 0 & \frac{5}{2} & 0 & 6 \\ \frac{4}{3} & 1 & 1 & 2 & -4 \\ 1 & -\frac{3}{2} & -\frac{9}{4} & -1 & 1 \end{pmatrix}$$

It can be observed from Eq. (35) that the eigenvectors behave as expected, and the odd numbered ones contain a nodal point at the middle. It is also possible to examine the frequency response of the reconstructed system to inspect the locations of poles and zeros.

Figure 3 indeed shows that the reconstructed structure has strong amplification levels at odd multiples of the basis frequency and complete attenuation at even multiples. The computed response agreed exactly with the desired form in Eq. (3) and with Eq. (20). The outcome of this reconstruction is examined for several cases in Table 1.

4.1 Toward a Continuous Mechanical Fourier Generator. In order to study the topology of a MFSG when the number of terms approaches infinity, the algorithm in Appendix B was run with $N=12$ (total $2N+1=25$DOF).

The stiffness and mass distributions along the structure seem smooth in this case (e.g., Fig. 4), as they appear for any realization with a large number of DOF. The smoothness of mass and stiffness distributions could possibly suggest that a continuous structure having the same properties can be realized.

To illustrate the topology and shape of the MFSG in this case, it was realized numerically by a conceptual torsional system. The masses are represented by the displacement of mass-balls from the axis of rotation, and the stiffness is inversely proportional to the spacing between the mass elements (see Eq. (34)). Two eigenvectors are depicted in Fig. 5 to demonstrate the spatial behavior of this system.

Figure 6 visually demonstrates the smooth distribution of mass. The response to torque excitation at the middle mass has, in this case, evenly spaced natural frequencies, as shown in Fig. 7. The zeros appear at even multiples of first natural frequency.

Numerical and analytical verifications have shown that the proposed algorithm works as expected and that a system with a large

Table 1 Values of springs and masses for the mechanical Fourier series generators supporting Eq. (34)

$2N+1$	3	5	7
$\frac{m_1}{m_{N+1}}$	$\frac{6}{5}$	$\frac{10}{7}$	$\frac{700}{429}$
$\frac{m_2}{m_{N+1}}$	1	$\frac{15}{14}$	$\frac{350}{297}$
$\frac{m_3}{m_{N+1}}$		1	$\frac{28}{27}$
$\frac{k_1}{\omega_0^2 m_{N+1}}$	$\frac{9}{5}$	$\frac{25}{7}$	$\frac{2450}{429}$
$\frac{k_2}{\omega_0^2 m_{N+1}}$	3	$\frac{45}{7}$	$\frac{350}{33}$
$\frac{k_3}{\omega_0^2 m_{N+1}}$		$\frac{15}{2}$	$\frac{350}{27}$
$\frac{k_4}{\omega_0^2 m_{N+1}}$			14

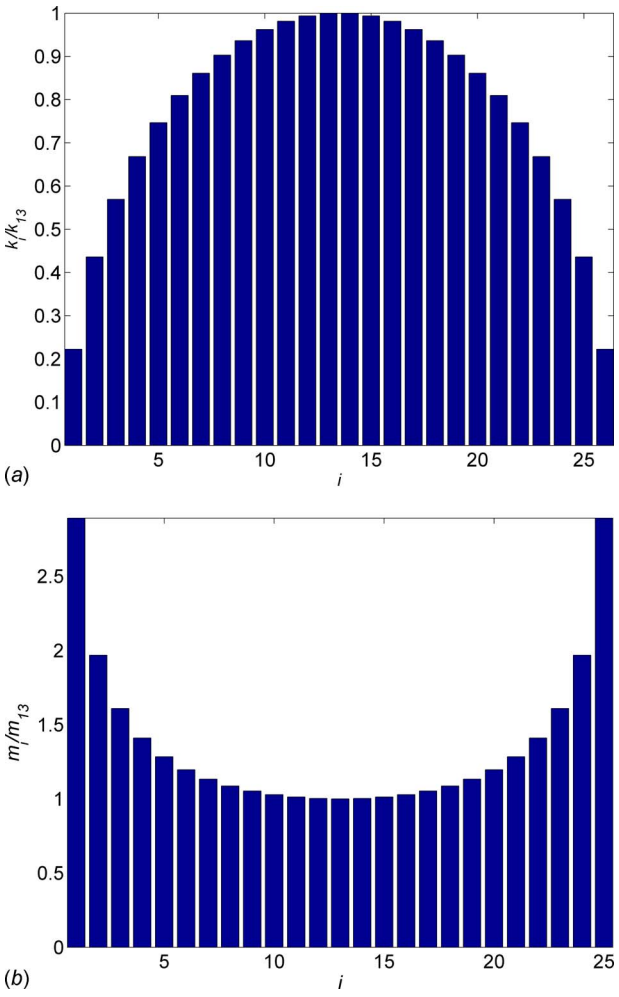

Fig. 4 Stiffness and mass elements for a 25DOF MFSG

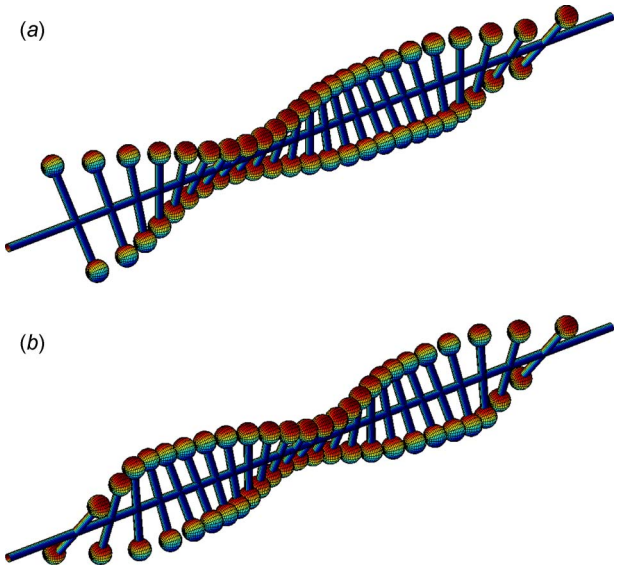

Fig. 5 Antisymmetric and symmetric eigenvectors of a 25DOF MFSG

number of degrees of freedom has smooth distributions of mass and stiffness.

To conclude the examples, a microscale realization of the MFSG is described.

4.2 Micromechanical Realization. A miniature system made of silicon has been designed and manufactured using micro electromechanical systems (MEMS) manufacturing techniques [15,17]. The structure operates in torsion and it is driven by means of a split electrode acting under the middle mass to create the excitation torque. A possible application of this device is to form an optical scanning mirror, as described in Ref. [14].

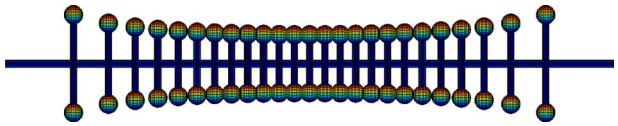

Fig. 6 Pictorial realization of a 25DOF MFSG

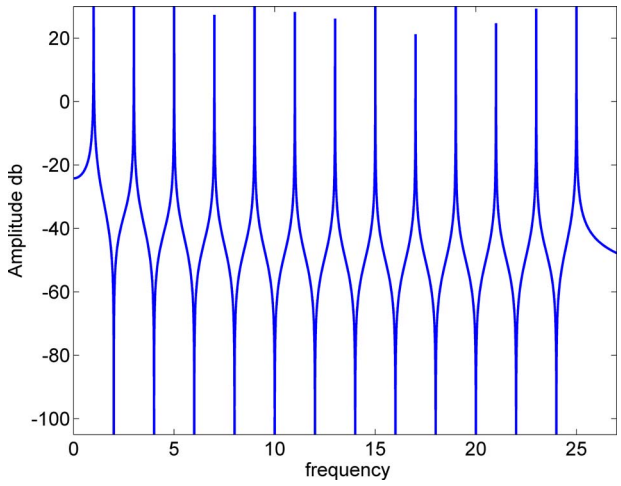

Fig. 7 Frequency response amplitude of a 25DOF MFSG

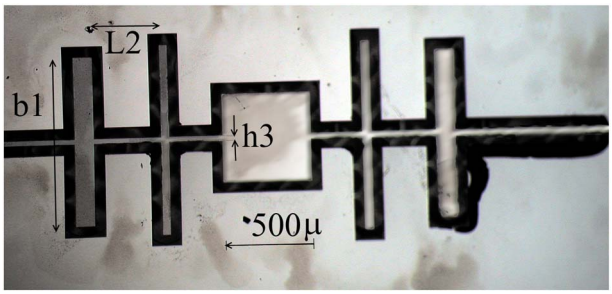

Fig. 8 Photograph of a miniature DFG

Modeling the springs as rectangular cross-section torsional beams and the masses as rectangular rigid plates with the same thickness as the beam yields the following expressions [18] for the stiffness and mass elements:

$$k_i = \frac{cGh_i^3 t}{L_i}, \quad m_i = \frac{a_i b_i t \rho (b_i^2 + t^2)}{12} \tag{36}$$

where c is the warping function correction coefficient [18], G is the material shear module, h_i is the individual beam's cross-section width, $t=30\mu$ is the structure's thickness, L_i is the individual beam length, a_i is the plate length (parallel to rotation axis), b_i is the plate width (perpendicular to the rotation axis), and ρ is the material density.

The structure is designed according to Eq. (36) and using the proposed algorithm under the constraints that $\omega_0=15{,}000$ Hz and the center mass is $m_3=500\mu\times500\mu\times\rho\times t$.

A photograph of the structure, taken under a microscope with the indication of the main dimensions, is shown in Fig. 8.

The structure was simulated by a finite element (FE) model created by the structural dynamics toolbox in MATLAB™ [19]. Two mode shapes that are plotted in Fig. 9 demonstrate that the structure does behave as a discrete 5DOF system and the rectangular plates do remain rigid.

Examining the left part of Fig. 9 it can be seen that the central mass does not move at this frequency ($4\omega_0$) despite the fact that the excitation operates at the same location. The right part of the figure shows an eigenvector ($5\omega_0$) that is symmetric.

Finally, a more visual validation showing that no other dynamics affect the MFSG uses a comparison of the computed and measured frequency response functions in Fig. 10.

Clearly, the fabricated device shows a near perfect behavior and it agrees well with the simulated model. The accuracy of the obtained natural frequencies is affected by manufacturing tolerances, but still an agreeable accuracy was obtained here. The problem of accommodating manufacturing tolerances is treated in some detail in Ref. [15]. More details about the manufacturing process are provided in Ref. [17].

5 Conclusion

An inverse problem allowing designers to create vibrating structures that can produce a periodic nonsinusoidal response with small power consumption was described. The proposed structure requires a small excitation torque and power as it amplifies all the discrete spectral lines that appear in the response while attenuating other spectral contents. In addition to setting the natural frequencies at desired locations, the algorithm chooses frequencies where the excitation would be attenuated; these frequencies (even multiples) often appear in electrostatic and electromagnetic systems as parasitic terms. It was demonstrated that the algorithm leads to mechanical systems having smooth distributions of mass and stiffness when the number of degrees of freedom becomes high and it suggests that a continuous implementation can be a viable option. A small micromechanical device was manufactured

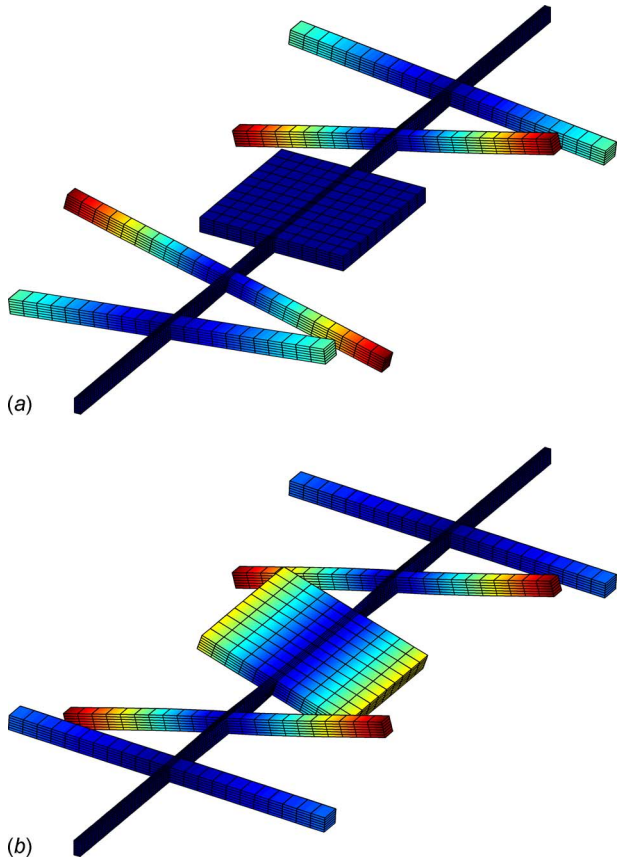

Fig. 9 Antisymmetric (left) and symmetric (right) modes of the miniature structure FE model

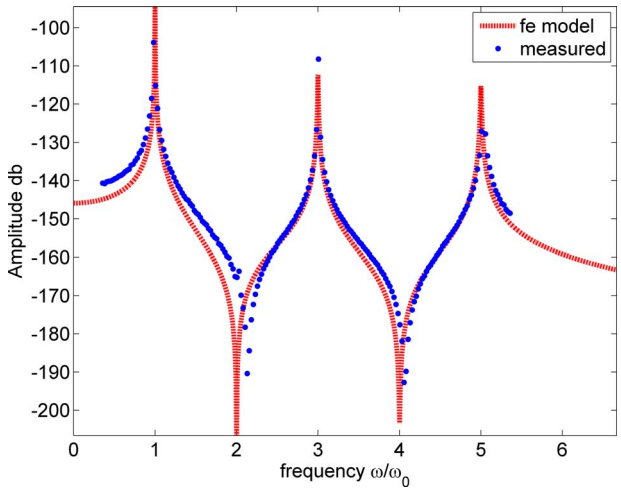

Fig. 10 Measured and computed by finite element and frequency response amplitude

according to the present algorithm proving the theory, thus showing possible applications as an optical scanning device.

Appendix A: Proof of Eq. (25)

This appendix proves Eq. (25) in a slightly different way than previous references (i.e., Refs. [12,4]).

Considering the eigenvalues of M_1, K_1 can be expressed with Eq. (24) as

$$(\lambda_i I - B)u_i = 0 \tag{A1}$$

Since B is symmetric, $U=(u_1\ u_2 \cdots u_{N+1}) \in \mathbb{R}^{(N+1)\times(N+1)}$ is orthogonal, and thus we have $U^T U = I$ and $U^{-1} = U^T$. U contains the eigenvectors of B as its columns.

Using the spectral decomposition of B, it is possible to express the resolvent as

$$(\lambda_i I - B)^{-1} = (\lambda_i I - U\Lambda U^T)^{-1} = (U(\lambda_i I - \Lambda)U^T)^{-1} = U(\lambda_i I - \Lambda)^{-1}U^T \tag{A2}$$

with

$$(\lambda_i I - B)^{-1} = \frac{1}{|\lambda_i I - B|}\mathrm{adj}(\lambda_i I - B) \tag{A2'}$$

One can write

$$\mathrm{adj}(\lambda_i I - B) = |\lambda_i I - B|(\lambda_i I - B)^{-1} = \left(\prod_{k=1}^{N+1}(\lambda_i - \lambda_k)\right)U(\lambda_i I - \Lambda)^{-1}U^T \tag{A3}$$

or

$$\mathrm{adj}(\lambda_i I - B) = \left(\prod_{k=1}^{N+1}(\lambda_i - \lambda_k)\right)\left(\sum_{p=1}^{N+1}\frac{1}{(\lambda_i - \lambda_p)}u_p u_p^T\right) \tag{A4}$$

and

$$\mathrm{adj}(\lambda_i I - B) = \left(\prod_{k=1}^{N+1}(\lambda_i - \lambda_k)\right)\left(\sum_{\substack{p=1 \\ p\neq i}}^{N+1}\frac{1}{(\lambda_i - \lambda_p)}u_p u_p^T\right) = \prod_{\substack{k=1 \\ k\neq i}}^{N+1}(\lambda_i - \lambda_k)u_i u_i^T \tag{A5}$$

Now treat the $(N+1,N+1)$th element of the left hand side of Eq. (A5). Indeed the $(N+1,N+1)$th element of $\mathrm{adj}(\lambda_i I - B)$ is computed by taking the determinant of this matrix with the $(N+1)$th row and column removed and therefore let B_0 consist of the first N rows and columns of B. Thus,

$$|\lambda_i I - B_0| = \prod_{k=1}^{N}(\lambda_i - \mu_k) \tag{A6}$$

Substituting Eq. (A6) into $(N+1,N+1)$th entry of Eq. (A5),

$$\prod_{k=1}^{N}(\lambda_i - \mu_k) = \prod_{\substack{k=1 \\ k\neq i}}^{N+1}(\lambda_i - \lambda_k)u_i^2(N+1) \tag{A7}$$

and finally the

$$u_i^2(N+1) = \frac{\prod_{k=1}^{N}(\lambda_i - \mu_k)}{\prod_{\substack{k=1 \\ k\neq i}}^{N+1}(\lambda_i - \lambda_k)}, \quad i = 1, \ldots, N+1 \tag{A8}$$

Relating the eigenvalues of B and B_0 to those of M, K it is clear that Eq. (A8) is identical to Eq. (25). Therefore Eq. (A8) can be used to retrieve $u_i^2(N+1)$, which is the $(N+1)$th column of $L = U^T$ (also known as the left eigenvector matrix or the reciprocal base).

Appendix B: MATLAB Programs

This appendix lists several MATLAB™ programs that realize the proposed algorithm. One should run part i that calls other subprograms that listed below.

```
%Part i–Complete reconstruction—calls other sub-programs
N=2;                                                    % Fourier series would have 2N+1 terms
lambda2n=sym([1:2:2*N+1].^2);                           %N+1 poles—at odd multiples
mu=sym([2:2:2*N].^2);                                   % N zeros—at even multiples
[u_N]=compute_un(lambda2n,mu);                            % compute vector
[bn,an,x]=reverse_lanczos(u_N,lambda2n);                  % compute diagonals of Jacobi matrix
B=diag(an)-diag(bn,1)-diag(bn,-1);                      % form Jacobi matrix
[M,K,m0,k0]=jacobi_to_mk(B);                            % convert to M,K

    m_Np1=1;  ω0=2*pi*15000;                            %scaling, central mass m(N+1) and w0 [Rad/s]
    temp=M(N+1,N+1); M=M*m0(N+1)/temp; K=K*ω0^2/temp; % apply scaling
[Phi  w2]=eig(M\K);                                     % compute eigenvalues/vectors to verify
Frequencies_Hz=sqrt(diag(w2))/2/pi                      % convert eignevalues to frequencies in Hz
```

```
% Part ii—implement Eq. (25)
function [u_N]=compute_un(lambda,mu)
Np1=length(lambda);                                     %N+1, no. of eigenvalues in M1, Eq. (21)
For i=1:Np1
j=1:Np1; j(i)=[ ];                                      % indices vector, enforce j<>i
u_N_squared2(i)=prod(mu-lambda(i))/prod(lambda(j)-lambda(i));
end
u_N=sqrt(u_N_squared2);
```

```
% Part iii - reconstruct the B-Jacobi matrix using the
% Lanczos algorithm [4] (Eq. 4.2.12-Eq. 4.2.17)

function [bn,an,x]=reverse_lanczos(u_N,lambda)

Np1=length(lambda); N=Np1-1; %N+1 and N, eigenvalues of B
x=sym (zeros(Np1));
x(:,Np1)=u_N(:);                                        %make vector a column (u_N);
an(Np1)=sum(lambda.*u_N.^2);                            %x(N).'*diag(p)*x(N)
dN=an(Np1)*x(:,Np1)-diag(lambda)*x(:,Np1);
bn(N)=sqrt(sum(dN.*dN));
x(:,N)=dN/bn(N);
for i=N:-1:2
    an(i)=x(:,i).'*diag(lambda)*x(:,i);
    d=an(i)*x(:,i)-diag(lambda)*x(:,i)-bn(i)*x(:,i+1);
    bn(i-1)=sqrt(sum(d.*d));
    x(:,i-1)=d/bn(i-1);
end
an(1)=x(:,1).'*diag(lambda)*x(:,1);
```

```
% Part iv–convert Jacobi matrix to Mass and Stiffness of Fig. 1
function [M,K,m0,k0]=jacobi_to_mk(B)
% M,K–realization of Fig. 1
% m0,k0–reconstructed mass and stiffness elements
Np1=size(B,1); N=Np1-1;
t=inv(B);
t=t(1,:).';                                             % see Eq. (29)
    K=sym(zeros(2*N+1));
    M=sym(zeros(2*N+1));
    M(1:Np1,1:Np1)=diag(t.^2);                          % Eq. (30)
  % see Fig. 2 and Fig. 1—make M from two halves
M(Np1:2*Np1-1,Np1:2*Np1-1)=M(Np1:2*Np1-1,Np1:2*Np1-1)+diag(flipud(t.^2));
    K0=diag(t)*B*diag(t);                               % Eq. (31)
K(1:Np1,1:Np1)=K0;
K(Np1:2*Np1-1,Np1:2*Np1-1)=K(Np1:2*Np1-1,Np1:2*Np1-1)+K0(Np1:-1:1,Np1:-1:1);
%% compute spring and mass elements
    E1=triu(ones(Np1)); % inverse of E                  % see Eq. (24)
                                                        %K0=E'*Kv*E-->Kv=inv(E.')*K0*inv(E); Eq. (24)
k0=E1*K0*E1.';                                          inverted
k0=diag(k0);                                            % diagonal of springs
k0=[k0;k0(end:-1:1)];                                   % complement second half, Fig. 2→Fig. 1
m0=sym(zeros(2*N+1,1));
m0(1:Np1)=t.^2;m0(Np1:end)=m0(Np1:end)+flipud(t.^2);
```

• Comment:

The same algorithm can support Fourier series consisting of both odd and even multiples of the basis frequency. As an example, use these lines to obtain the desired natural frequencies

```
N=2;                                                    % choose any even value for N
lambda=sym([1:1:N+1]).^2);                              % poles
mu=sym([3/2:1:N+1]).^2);                                % zeros
```

References

[1] Geradin, M., and Rixen, D., 1997, *Mechanical Vibration Theory and Application to Structural Dynamics*, Wiley, New York.

[2] Gabay, R., and Bucher, I., 2006, "Resonance Tracking in a Squeeze-Film Levitation Device," Mech. Syst. Signal Process., **20**(7), pp. 1696–1724.

[3] Boley, D., and Golub, G., 1987, "A Survey of Matrix Inverse Eigenvalue Problem," Inverse Probl., **3**, pp. 595–622.

[4] Gladwell, G. M., 1986, *Inverse Problems in Vibration*, Martinus Nijhoff, Dordrecht.

[5] Mottershead, J. E., 2001, "Structural Modification for the Assignment of Zeros Using Measured Receptances," Trans. ASME, J. Appl. Mech., **68**(5), pp. 791–798.

[6] Kyprianou, A., Mottershead, J. E., and Ouyang, H., 2005, "Structural Modification, Part 2: Assignment of Natural Frequencies and Antiresonances by an Added Beam," J. Sound Vib., **284**(1–2), pp. 267–281.

[7] Bucher, I., and Braun, S., 1993, "The Structural Modification Inverse Problem: An Exact Solution," Mech. Syst. Signal Process., **7**(3), pp. 217–238.

[8] Kailath, T., 1980, *Linear Systems*, Prentice-Hall, Englewood Cliffs, NJ.

[9] Ewins, D. J., 2000, *Modal Testing: Theory, Practice, and Application*, Research Studies Press, Baldock, England.

[10] Gantmakher, F., and Krein, M., 1950, *Oscillation Matrices and Kernels and Small Vibrations of Mechanical Systems*, State Publishing House for Technical-Theoretical Literature, Moscow-Leningrad.

[11] Lanczos, C., 1950, "An Iteration Method for the Solution of the Eigenvalue Problem of Linear Differential and Integral Operators," J. Res. Natl. Bur. Stand., **45**, pp. 225–232.

[12] Hochstadt, H., 1979, "On the Reconstruction of Jacobi Matrix From Spectral Data," Linear Algebr. Appl., **8**(5), pp. 435–446.

[13] Cantoni, A., and Butler, P., 1976, "Properties of the Eigenvectors of Persymmetric Matrices With Applications to Communication Theory," IEEE Trans. Commun.," **24**(8), pp. 804–809.

[14] Bucher, I., Avivi, G., and Velger, M., 2004, "Design and Analysis of Multi Degrees of Freedom Micro-Mirror for Triangular-Wave Scanning," Proc. SPIE, **5390**, pp. 410–420.

[15] Avivi, G., and Bucher, I., 2008, "A Method for Eliminating the Inaccuracy of Natural Frequency Multiplications in a Multi DOF Micro Scanning Mirror," J. Micromech. Microeng., **18**(2), p. 025028.

[16] Bishop, R. E., Gladwell, G. M., and Michaelson, S., 1979, *The Matrix Analysis of Vibration*, Cambridge University Press, Cambridge.

[17] Elka, A., and Bucher, I., 2008, "On the Synthesis of Micro-Electromechanical Filters Using Modes Shapes," J. Micromech. Microeng., **18**(12), p. 125018.

[18] Timoshenko, S., and Goodier, J., 1970, *Theory of Elasticity*, McGraw-Hill, New York.

[19] Balmes, E., 2008, "Structural Dynamics Toolbox for Use With MATLAB," http://www.sdtools.com.